Helical Structure and Folding of Subunit *c* of F_1F_o ATP Synthase: ^1H NMR Resonance Assignments and NOE Analysis†

Mark E. Girvin and Robert H. Fillingame*

Department of Biomolecular Chemistry, University of Wisconsin, Madison, Wisconsin 53706

Received May 28, 1993; Revised Manuscript Received August 23, 1993®

ABSTRACT: Subunit *c* of the H^+-transporting F_1F_o ATP synthase (EC 3.6.1.34) is thought to fold across the membrane as a hairpin of two α-helices and function as a key component of the H^+-translocase of F_o. We report here the initial results of a structural study of purified subunit *c* in a chloroform–methanol–water (4:4:1) solvent mixture using standard two-dimensional NMR techniques. The spin systems of 78 of the 79 amino acid side chains have been assigned to residue type, and 44 of these have been assigned to specific residues in the sequence. Stretches of α-helical secondary structure were observed for Asp7–Ile26 in the first proposed transmembrane helix, and for Arg50–Ile55 and Ala67–Val78 in the second proposed transmembrane helix. Nuclear Overhauser effects (NOEs) were observed between residues at both ends of the predicted transmembrane helices. The intensities of the NOEs between helix-1 and helix-2 were not diminished by mixing of ^2H-subunit *c* with ^1H-subunit *c*, and therefore the NOEs must be due to intramolecular, rather than intermolecular, interactions. Hence the purified protein must fold as a hairpin in this solvent system, just as it is thought to fold in the lipid bilayer of the membrane. In native F_o, dicyclohexylcarbodiimide reacts specifically with Asp61 in the second transmembrane helix of subunit *c*, and the rate of this reaction is reduced by substitution of Ile28 by Thr on the first transmembrane helix. The I28T substitution is shown here to alter the chemical shifts of protons at and around Asp61. This observation provides a further indication that subunit *c* may fold in chloroform–methanol–water solvent much like it does in the membrane.

The final step of oxidative phosphorylation and photophosphorylation is catalyzed by a reversible H^+-transporting ATP synthase. This enzyme catalyzes the synthesis of ATP from ADP and P_i as protons are transported down a transmembrane, electrochemical H^+ gradient formed by the electron transport complexes. The ATP synthase is composed of two moieties termed F_1 and F_o. Synthesis of ATP occurs in the membrane extrinsic F_1 sector, which functions as an ATPase when it is removed from transmembrane F_o sector. The translocation of protons through the membrane is accomplished by the membrane intrinsic F_o sector. When F_1 is bound to F_o, the translocation of protons through F_o is reversibly coupled to ATP synthesis by F_1 (Senior 1988).

The F_o sector is composed of three subunits *a*, *b*, and *c* in a stoichiometry of 1:2:10 (Foster & Fillingame, 1982). Each subunit is thought to span the membrane, (Fillingame, 1990), and all three are required in reconstitution of a functional F_o (Schneider & Altendorf, 1985). Subunit *c* appears to play a role in both H^+ translocation and the coupling of H^+ translocation to ATP synthesis on F_1 (Senior, 1988; Fillingame, 1990).

Subunit *c* is a small (79-residue) protein which has been proposed to fold in the membrane as a hairpin with two hydrophobic α-helices connected by a more polar loop. The polar loop is exposed on the F_1 binding side of the membrane (Girvin et al., 1989; Hensel et al., 1990). Genetic evidence suggests that the polar loop, and in particular the conserved Arg-Gln-Pro sequence, is important for the binding and proper coupling of F_1 to F_o (Mosher et al., 1985; Miller et al., 1989; Fraga & Fillingame, 1989). A conserved carboxyl group (Asp61 in the *Escherichia coli* protein) located in the middle of the C-terminal membrane-spanning sequence has been shown to be essential for H^+ translocation. Specific modification of this residue by DCCD,[1] or substitution by Gly or Asn, abolishes both H^+ translocation and ATP synthesis (Hoppe & Sebald, 1984; Fillingame, 1990). The protein is thought to fold in the membrane as a hairpin such that Asp61 of helix-2 lies close to Ala24 and Ile28 of helix-1. This folding model is supported by the analysis of several types of mutants. Mutation of Ala24 or Ile28 alters the reactivity of Asp61 with DCCD (Hoppe et al., 1980; Fillingame et al., 1991). Further, Miller et al. (1990) have shown that the essential carboxyl group can be moved from position 61 of helix-2 to position 24 of helix-1 in a D24G61 double mutant with retention of function. That is, residue 61 and residue 24 must lie close enough to each other to accommodate the anchoring of the carboxyl group at an equivalent position in the membrane.

We have initiated a study of purified subunit *c* by NMR in the hope that the structural information will provide insights into the mechanism of H^+ translocation and the mode of coupling to ATP synthesis. This paper addresses the overall folding of purified subunit *c*. ^1H NMR assignments for 44 of the 79 residues in the protein are presented together with information on the secondary structure of the protein.

† This study was supported by U.S. Public Health Service Grant GM23105 from the National Institutes of Health. M.E.G. was partially supported by U.S. Public Health Service Fellowship Award F32-GM11096 during the initial phase of the work. The National Magnetic Resonance Facility at Madison, supported by NIH Grant RR02301, was used in these studies. Equipment in the facility was purchased with funds from the University of Wisconsin, the NSF Biological Instrumentation Program (Grant DMB8415048), NIH Biomedical Research Technology Program (Grant RR02301), NIH Shared Instrumentation Program (Grant RR02781), and the U.S. Department of Agriculture.

® Abstract published in *Advance ACS Abstracts*, October 15, 1993.

[1] Abbreviations: *atp*, operon for eight genes coding ATP synthase subunits (formerly called *unc* operon); 2D, two dimensional; 3D, three dimensional; COSY, 2D correlated spectroscopy; DCCD, *N,N'*-dicyclohexylcarbodiimide; DQF, double quantum filtered; NCCD, *N*-(2,2,6,6-tetramethyl-*N*-oxy-1-piperidyl)-*N'*-cyclohexylcarbodiimide; NOE, nuclear Overhauser effect; NOESY, 2D NOE spectroscopy; TMS, tetramethylsilane; TOCSY, 2D total correlation spectroscopy.

0006-2960/93/0432-12167$04.00/0

Interactions between the two proposed membrane-spanning helices are demonstrated in solution, both from NOE measurements and from the transhelical effects of mutations and chemical modification by DCCD.

EXPERIMENTAL PROCEDURES

Isolation of Subunit c. Wild-type subunit *c* was purified from several strains of *E. coli* after overexpression. F_1F_o was overexpressed in strain MM598 by heat induction of a λ-*atp*$^+$ lysogen as described in Hermolin et al. (1983). Strain LW99 is a transformant of plasmid pAP55 (Porter et al., 1983), which carries the *atp*$^+$ (ATP synthase) operon coding each of the F_1F_o genes in wild-type strain JM83 (Messing & Vieira, 1982). Strain LW99 overproduces F_1F_o to 3–5 times the monoploid level. Strain OM241 contains a plasmid carrying the gene for subunit *c* (plasmid pCP35; Fillingame et al., 1991) in a chromosomal background where the *atp* was deleted [*atp*(ΔB-C) deletion (Klionsky et al., 1983)]. The *atp* deletion was transduced with Asn$^+$ into strain ER (Felton et al., 1980) prior to transformation with plasmid pCP35. Subunit *c* was produced at 6–8 times the monoploid level in strain OM241 in the absence of other F_1F_o subunits. The DCCD resistant mutant proteins I28T (Hoppe et al., 1980) and A24S (Fillingame et al., 1991) were prepared from monoploid strains DC25 and RF7, respectively, after growth of cells on a combination of succinate, malate, and acetate as the carbon sources (Fillingame, 1975).

Uniformly deuterated subunit *c* was isolated from the overproducing strain MEG119 (plasmid pCP35 in strain ER made Asn$^+$) grown on 0.5% [^{2}H]acetate in ^2H_2O, both isotopically enriched to a level of 99.8%. Growth was very slow under these conditions, with a doubling time of 20 h, but typical cell growth yields and subunit *c* overproduction were obtained.

Subunit *c* was extracted from whole cells of the above strains with chloroform–methanol (2:1), and the extract was concentrated and then precipitated with diethyl ether as described (Fillingame, 1976; Beechey et al., 1979). It was further purified from the chloroform–methanol extract by CM-cellulose chromatography (Graf & Sebald, 1978; Hermolin & Fillingame, 1989), where 1.0 mL of CM-cellulose bed volume was used for each milligram of ether-precipitated protein. A modified Lowry assay that included SDS was used to estimate protein concentration using bovine serum albumin as a standard (Fillingame, 1975). The values obtained for purified subunit *c* were multiplied by a factor of 1.97 to correct for low color development of subunit *c* relative to serum albumin (Fillingame, 1976; Hermolin & Fillingame, 1989).

DCCD-modified subunit *c* was prepared after reaction of DCCD with subunit *c* in the isolated membrane. Membranes, prepared from strain LW99 cells according to Hermolin et al. (1983), were suspended at 25 mg/mL membrane protein in TMDG buffer [50 mM Tris-HCl, 5 mM $MgCl_2$, 1 mM dithiothreitol, 10% (v/v) glycerol, pH 7.5], and treated with 100 μM DCCD for 2.5 h at 30 °C. The protein was then extracted and purified on CM-cellulose as described, and the modified and unmodified forms of the protein were separated by DEAE-cellulose chromatography using an ammonium acetate gradient in chloroform–methanol–H_2O (4:4:1) (Fillingame, 1976; Beechey et al., 1979).

Sample Preparation for NMR Spectroscopy. Samples of subunit *c* in deuterated solvent were prepared by evaporation of [^{1}H]chloroform–methanol solvent and gradual dilution into ^{2}H solvent mixtures. A 4–8-mg sample of subunit *c* [dissolved at ca. 2 mg/mL in chloroform–methanol (2:1)] was dried to ≤0.1 mL in a round-bottomed 25-mL tube under a stream of argon, with the addition of C^2HCl_3 as necessary to keep the protein dissolved. A volume of 1.0 mL of C^2HCl_3–$C^2H_3O^2H$ (2:1) was added to the sample, and the sample was dried again to ≤0.1 mL under argon. This process was repeated one or two more times to remove most of the ^{1}H solvent.[2] The protein was then taken to dryness and redissolved in 0.5 mL of C^2HCl_3–$C^2H_3O^2H$–^2H_2O (4:4:1) with NaCl added to a final concentration of 50 mM. The sample was filtered using 0.45-μm fluoropolymer filters (Gelman, Ann Arbor, MI), and TMS was added as the reference. The final protein concentration was 1–2 mM (8–16 mg/mL). The pH of the sample was adjusted prior to the transfer to ^{2}H solvent and was remeasured in the final 0.5-mL sample volume. All chemical shifts are reported for the protein at pD 6.8. Spectra at pD 4.2 were used for verifying H^N–H^N NOE assignments.

NMR Spectroscopy. All two-dimensional NMR spectra were acquired at 27 °C on a Bruker AM-500 spectrometer. Phase-sensitive DQF COSY experiments were performed according to Rance et al. (1983). The TOCSY experiment employed the 90_x–t_1–SL_x–MLEV17–SL_x–acquisition sequence, described by Bax and Davis (1985), where SL_x is a 2-ms trim pulse and MLEV17 is the composite pulse sequence repeated for 18–28 cycles in different experiments to give mixing times of 55, 75, and 90 ms. NOESY data were acquired with the 90_x–t_1–90_x–t_m–90_x–acquisition sequence (Kumar et al., 1980; Bodenhausen et al., 1984) with a 100-, 150-, or 200-ms mixing time, randomly varied by 20 ms to reduce scalar coupling effects (Macura et al., 1982).

Data were acquired on an Aspect 3000 computer as 480–512 blocks of 64–128 transients, each with 4096 time domain points. Sweep widths were typically 5319 Hz, and the relaxation delay was 2.0 s. The data in the figures shown were processed on an IBM AT compatible computer using Felix PC software (Hare Research, Bothell, WA). The data sets were zero filled to 4096 × 2048 ($t_2 \times t_1$) data points and multiplied by shifted sine bell window functions in both dimensions before Fourier transformation. All chemical shifts are expressed relative to TMS.

RESULTS

Selection of Solvent for NMR Spectroscopy. Since subunit *c* is ordinarily purified in chloroform–methanol (2:1), this was an obvious first choice as the solvent for the NMR experiments. However, a concentration-dependent broadening of the NMR resonances occurred over the range of 0.1–2.5 mM subunit *c* in chloroform–methanol (2:1), suggesting that the protein was aggregating under these conditions. The aggregation was abolished by the addition of water and salt to the solvent. In chloroform–methanol–water (4:4:1) made 50 mM in NaCl, no detectable broadening of the resonances occurred over a range of protein concentration of 0.1–2.5 mM, and this was chosen as the standard solvent system.

Side-Chain Spin System Assignments. The first step in the now-standard assignment strategy described by Wüthrich (1986) is assignment of spin system resonances to residue type. All but one of the 79 pairs of αβ protons (αα′ for Gly) were resolved in COSY type experiments, and all of these have been assigned to residue or spin system type. The single, missing system was of the Glu/Gln/Met type. All spectra

[2] The procedure described for gradual dilution of ^{1}H solvent proved necessary. When the protein in [^{1}H]chloroform–methanol was taken to complete dryness in one step, it was very difficult to redissolve in [^{2}H]-chloroform–methanol–water. This procedure was also required to minimize the residual ^{1}H solvent resonances.

Table I: ^{1}H Resonance Assignments for Subunit *c*

residue	H^N	H^α	H^β	H^γ	H^δ and other	residue	H^N	H^α	H^β	H^γ	H^δ and other
Ala12		4.03	1.33			Leu70	8.72	4.26	1.70	1.87	0.94, 0.91
Ala13	8.29	4.04	1.55			Leu72	8.42	4.11	2.19, 1.61	1.91	0.94, 0.91
Ala14	8.32	4.14	1.62			LeuA		3.55	2.09		1.09, 0.95
Ala24	8.14	4.08	1.65			LeuB		3.64	2.15		1.17, 1.07
Ala25	8.48	4.20	1.58			LeuC		3.73	2.05, 1.98		0.88, 0.77
Ala62		4.29	1.58			LeuD		3.79	2.02, 1.94	1.84	0.99, 0.87
Ala67	8.33	4.04	1.55			LeuE		3.84	2.08		0.94
Ala77		4.12	1.28			LeuF		3.86	2.25		0.96
AlaA		4.25	1.44			LeuG		4.00	1.98, 1.66		0.98
AlaB		4.35	1.45			LeuH	7.98	4.14	1.89	1.78	0.92
AlaC		4.14	1.49			LeuI		4.22	2.12	1.72	1.01, 0.95
AlaD	8.45	4.04	1.59			Lys34		4.24	2.12	1.55	1.71; ϵ: 2.89
AlaE	8.26	4.16	1.64			Met11	8.24	4.46	2.03, 2.15	2.58, 2.64	
Arg41		4.33	1.87	1.69, 1.83	3.19; NH: 7.68	Met16		4.57	2.07, 2.42	2.23	
Arg50		3.97	1.92	1.62, 1.83	3.16; NH: 7.47	Met17	8.34	4.17	2.19, 2.31	2.61, 2.76	
Asp7		4.46	2.82, 3.14			Met75	8.03	4.00	2.15, 2.24	2.35, 2.51	
Asp44		4.52	2.82, 3.15								
Asp61		4.59	2.84, 3.03			Phe35		4.29	3.29, 3.36	2,6H: 7.25	3,4,5H: 7.09
AsnA		4.45	2.73, 2.87			Phe53		4.14	3.04, 3.20	2,6H: 7.02	3,4,5H: 7.21
AsnB		4.58	2.73, 2.85			Phe54	8.06	4.18	3.31	2,6H: 7.37	3,4,5H: 7.29
Gln52[a]		3.89	1.97, 2.20	2.45	NH: 7.74	Phe76	8.11	4.38	3.17, 3.07	2,6H: 7.31	3,4,5H: 7.19
Gly18	8.59	4.18, 4.35				Pro64[a]		4.29	1.93, 2.33	2.26	3.86
Gly23	8.48	3.78, 3.89				ProA		4.21	1.72	2.04, 2.37	3.67
Gly58[a]		4.20, 4.43				ProB		4.41	1.95, 2.32	2.03, 2.07	3.72
Gly69	7.89	3.68, 3.90				Thr51		4.00	4.41	1.35	
Gly71	8.24	3.88, 4.15				Tyr10	8.25	4.21	3.07, 3.18	2,6H: 7.10	3,5H: 6.73
GlyA		3.74, 4.24				Tyr73	8.13	4.14	3.22, 3.36	2,6H: 7.04	3,5H: 6.71
GlyB		3.79, 4.42				Val15	8.34	3.71	2.28	1.14	
GlyC		3.92, 4.03				Val56	8.17	3.55	2.08	0.94, 1.09	
GlyD		3.97, 4.21				Val60	8.24	3.72	2.23	1.01, 1.08	
GlyE		4.00, 4.14				Val68	8.05	3.76	2.23	1.01, 1.17	
Ile22	8.21	3.76	1.95	1.59, 1.30, 1.09	0.85	Val74	8.35	3.52	2.27	0.98, 1.20	
Ile55	8.57	3.75	2.05	1.82, 1.24, 1.15	0.87	Val78		3.90	2.27	0.93	
IleA			1.81	1.63, 1.58, 1.05	0.81	Met/Gln/Glu					
IleB		3.45	1.77	1.65, 1.17	0.52	A		4.02	2.25, 2.36	2.51	
IleC		3.51	2.27	1.58, 1.39	0.94	B		4.03	2.33	2.64	
IleD		3.58	1.65	1.52, 1.22, 1.14	0.73	C		4.13	1.88, 2.04	2.61, 2.79	
IleE		4.10	1.91	1.83, 1.36, 1.26	0.79	D		4.15	2.24, 2.32	2.63, 2.79	
IleF		4.12	2.27	1.64, 1.29, 0.96	0.87	E		4.26	2.03, 2.11	2.56, 2.64	
Leu19	8.38	3.88	2.03			F		4.51	2.20, 2.30	2.77, 2.90	

[a] Assigned by loss of resonance in subunit *c* modified at Asp61 with a nitroxide analog of DCCD (see footnote 5 in text).

have been obtained in ^{2}H solvent mixtures because of the difficulties in suppressing multiple solvent ^{1}H resonances, and hence only the slowly exchanging H^N have been observed ($t_{1/2} > 1$ day). Remarkably, 35 of the 76 potentially observable H^N have been detected in ^{2}H solvent samples. A summary of the assignments is given in Table I.[3]

(a) Gly. All 10 Gly $\alpha\alpha'$ proton cross peaks were assigned from their position near the diagonal in the α proton region of the COSY spectrum (Figure 1). The only potential interference in this region of the spectrum would have been from the single Thr $\alpha\beta$ cross peak. However, the Thr resonances were easily distinguished and assigned. H^N resonances for 4 of the 10 Gly were assigned from COSY spectra (see Figure 6).

(b) Ala and Thr. All 13 Ala $\alpha\beta$ proton resonances clustered in the region of 4.0–4.35 ppm for the H^α and 1.2–1.7 ppm for the $(H^\beta)_3$ and were assigned (Figure 2). No further connectivities from the $(H^\beta)_3$ were seen in COSY and TOCSY spectra. The cross peak at 4.04, 1.55 ppm appears to arise from two separate Ala residues. Its intensity is greater than that of the other Ala cross peaks; it exhibits cross peaks to two H^N, and it is part of two separate NOESY connectivity sequences, as described later.

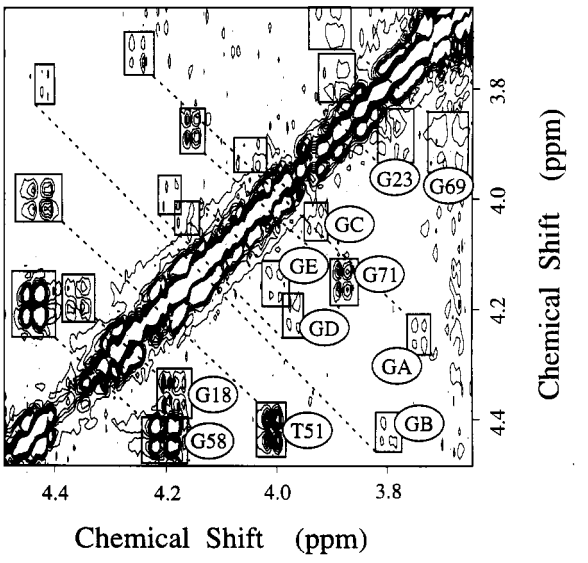

FIGURE 1: Contour plot of the Gly $\alpha\alpha'$ region of the 500-MHz ^{1}H DQF COSY spectrum of subunit *c*. The symmetric cross peaks on both sides of the diagonal are connected by dashed lines. The sample contained 2 mM subunit *c* in 4:4:1 C^2HCl_3–$C^2H_3O^2H$–^2H_2O, 50 mM NaCl, pD 6.8.

The sole Thr $\beta\gamma$ cross peak fell near the Ala at 1.35 ppm for the H^γ and 4.41 ppm for the H^β resonances (Figure 2). The Thr51 H^α was also easily distinguished at 4.00 ppm (Figure 1). The Thr51 H^N resonance was not observed.

[3] Most of the experiments reported here utilized subunit *c* purified from *E. coli* strains where the complete F_1F_o was overexpressed. However, when wild-type subunit *c* was overexpressed in the absence of other F_1F_o subunits and purified in chloroform–methanol solvent, the COSY spectra of the protein were identical to those shown here.

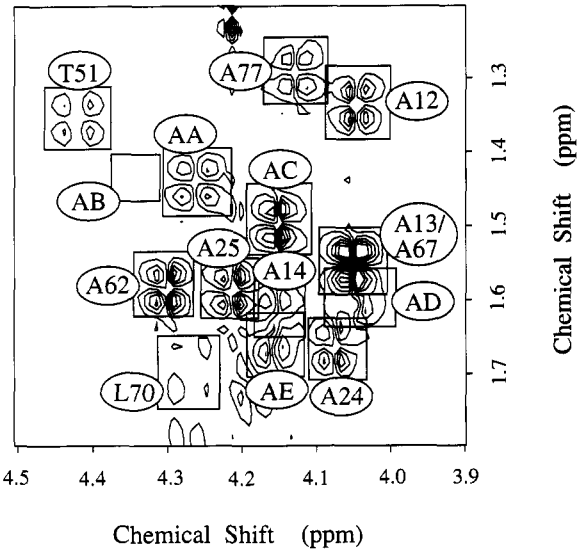

FIGURE 2: Expansion of the DQF COSY spectrum showing the Ala H^{α}–H^{β} and Thr H^{β}–H^{γ} cross peaks for wild-type subunit *c*. The missing cross peak labeled as AlaB could be seen at lower contour levels and was more pronounced in other COSY and TOCSY spectra.

(c) Val. The $\alpha\beta$ and $\beta\gamma$ cross peaks of four of the six Val were resolved in the COSY spectrum (examples of H^{β}–H^{γ} cross peaks are shown in Figure 3A). The remaining two Val had identical chemical shifts for the methine H^{β}, but were identified from TOCSY spectra (Figure 3B), and by modifications at Asp61 and Ile28, which shifted the H^{β} and H^{γ} of Val60. The amide protons of five of the Val were assigned from COSY spectra (not shown).

(d) Ile and Leu. Ile and Leu make up 25% of the residues in the protein and were among the most difficult to assign. Their side chains are lengthy, with several of the cross peaks occurring quite close to the diagonal, and the range of chemical shifts, particularly of the 12 Leu, is so small that there is drastic overlap in these regions of the 2D spectra (e.g., Figure 3A). We were able to resolve the δ-methyl protons for the Ile, and some of the Leu methyl protons in COSY spectra. The remainder of the side chains could only be resolved through the use of TOCSY spectra with several mixing times. Assignments for some of the $\alpha\beta$ cross peaks for both residue types have also been made from sequential NOESY backbone connectivities, as described later. The eight Ile $(H^{\gamma'})_2$ (1.1–1.4 ppm) to $(H^{\delta})_3$ (0.5–0.98 ppm) cross peaks were resolved in the COSY spectrum, as shown in Figure 3A. All of these side-chain assignments were extended using TOCSY spectra (Figure 3B). Seven of the twelve pairs of Leu H^{γ}–H^{δ} cross peaks were identified in the COSY spectrum (Figure 3A), and eleven of the side chains were resolvable in TOCSY spectra. The remaining assigned Leu are discussed in the section on sequential assignments.

(e) Lys and Arg. The $(H^{\delta})_2$–$(H^{\epsilon})_2$ cross peak of the unique Lys and the $(H^{\gamma})_2$–$(H^{\delta})_2$ cross peaks of the two Arg were well resolved in the COSY spectrum (not shown). The side chains of these residues could be traced back to their H^{α} in the TOCSY spectrum, as well as in the COSY spectrum for Arg41. Slowly exchanging amide protons were not observed for either of the two Arg or for Lys34.

(f) Pro. The three Pro residues were assigned from TOCSY spectra (not shown). In the case of ProA, a complete sequence of cross peaks from H^{α} through H^{δ} was present in the TOCSY spectrum (both with t_m = 75 and 90 ms). The other two Pro were assigned from separate sets of cross peaks from H^{α} to H^{β} and H^{γ}, and from H^{δ} to H^{γ} and H^{β}, in the 75- and 90-ms mixing time TOCSY spectra.

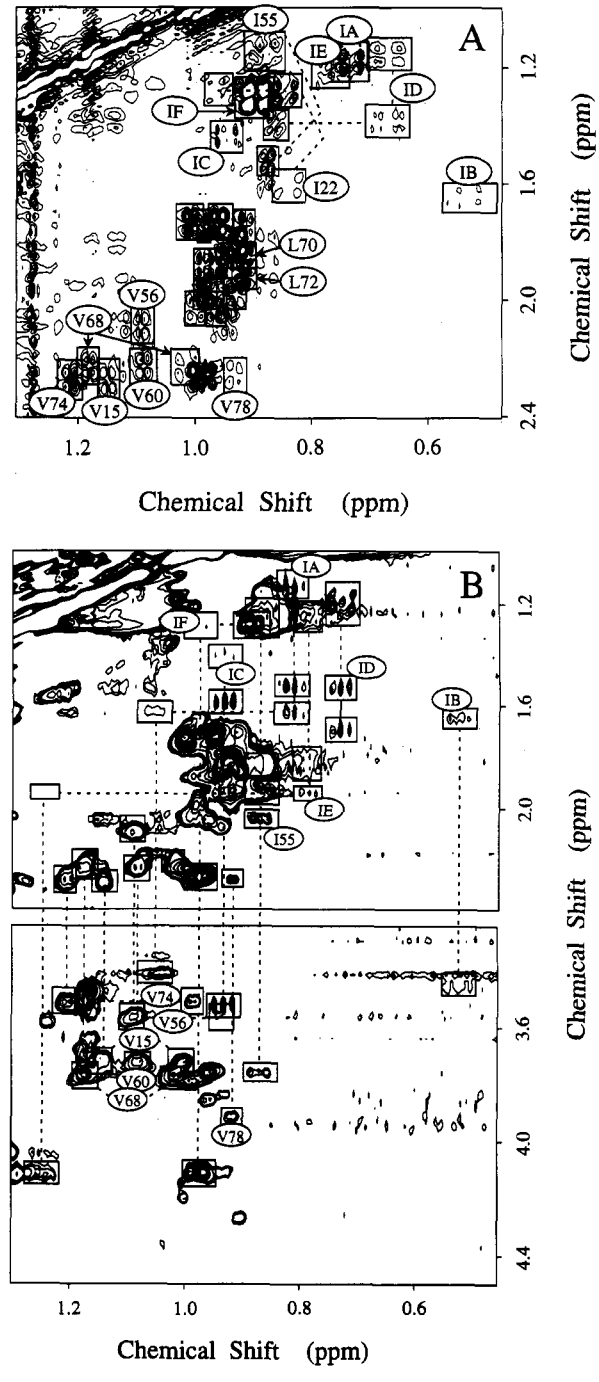

FIGURE 3: Expansions of DQF COSY and TOCSY spectra of subunit *c* showing the Val, Ile, and Leu methyl proton cross peaks. (A) Region of the DQF COSY showing Val H^{γ}–H^{β}, Ile H^{δ}–H^{γ} and H^{γ}–H^{β}, and Leu H^{δ}–H^{γ} methyl cross peaks. Some cross peaks are boxed but not labeled in crowded regions of the spectrum (e.g., the second methyl group of Val56, and most Leu cross peaks). For Ile55, cross peaks between the H^{δ} and both H^{γ} are observed, and for Ile22 and IleD, an additional cross peak to the $(H^{\gamma})_3$ is shown. (B) Region of the TOCSY spectrum (75-ms mixing time) showing the cross peaks from the methyl protons of Leu, Ile, and Val to all other side-chain protons of these residues. The crowded Leu region is not labeled.

(g) Asn, Asp, Phe, and Tyr. These four amino acids are treated together because of the similarities of both their $\alpha\beta$ proton chemical shifts and their spin system types. All four types of amino acid were readily visible in the COSY spectrum, with chemical shifts for the H^{α} of 4.1–4.6 ppm and for the $(H^{\beta})_2$ of 2.7–3.4 ppm (Figure 4A). When there was a cross peak from the H^{α} to only one of the two nonequivalent H^{β}, the other H^{β} was assigned from the COSY H^{β}–$H^{\beta'}$ cross peak near the diagonal (not shown).

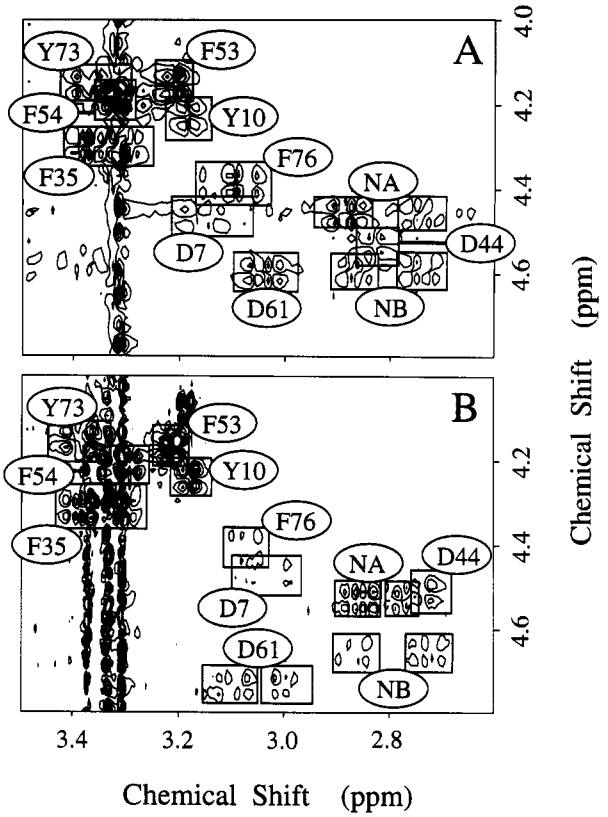

FIGURE 4: Expanded region of the DQF COSY spectrum of subunit *c*, illustrating the H^{α}–H^{β} cross peaks for Asp, Asn, Phe, and Tyr residues. (A) Wild-type and (B) DCCD-modified wild-type subunit *c*. Conditions as in Figure 1, except the concentration of the DCCD-modified protein was 1 mM.

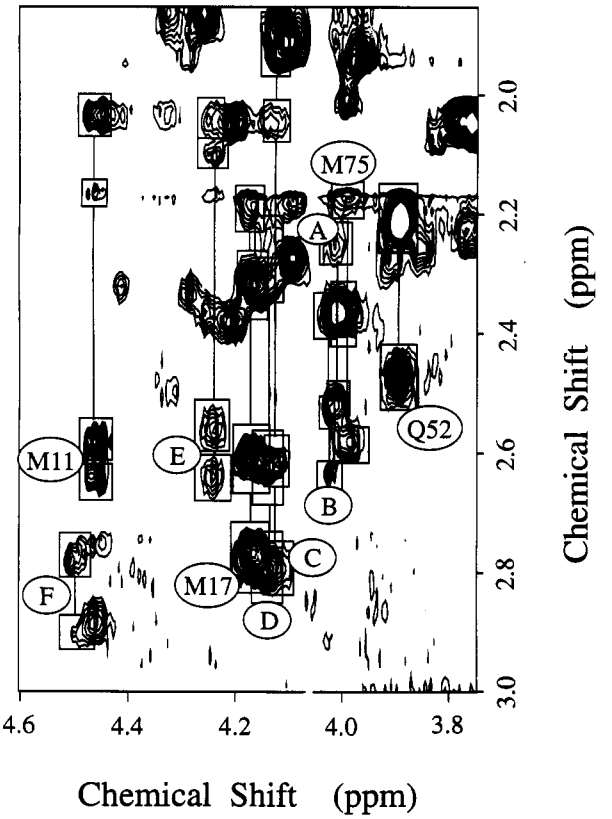

FIGURE 5: Expansion of the 75-ms TOCSY spectrum, showing the extended Met, Glu, and Gln correlations.

Phe and Tyr resonances were distinguished from each other and from those of Asp and Asn by the NOEs from their H^{α} and H^{β} to the aromatic ring protons at positions 2 and 6. These aromatic protons were readily resolved for the two Tyr and one of the four Phe in the COSY spectrum, and all were identified in TOCSY spectra. Each H^{β} and most H^{α} showed an NOE connectivity to a pair of aromatic protons. Several of the aromatic side chains exhibited additional interresidue NOEs, as discussed later. The H^{N} for both Tyr, and two of the Phe, were assigned from COSY spectra.

By process of elimination, the remaining five sets of $\alpha\beta$ proton cross peaks in the region belonged to the two Asn and three Asp residues in the protein. The Asp were later specifically assigned by other means.

(h) Met, Gln, and Glu. These three residue types were indistinguishable on the bases of spin system and typical chemical shifts. Analysis of COSY and especially TOCSY spectra yielded assignments for eleven H^{α}–H^{β}–H^{γ} sets for this type of spin system (Figure 5) out of the expected twelve (8 Met, 2 Glu, and 2 Gln). One Gln was assigned from the $H^{N\delta}$–$(H^{\beta})_2$ NOESY cross peak in ^1H solvent (data not shown), and four Met were assigned from sequential NOESY connectivities.

Sequence-Specific Assignments. The sequential assignment procedure relies on NOESY connectivities between backbone H^{N} and the H^{N}, H^{α}, and H^{β} of sequentially proximal residues. Almost half of the H^{N} of subunit *c* exchange very slowly with ^2H solvent. The first step was to assign the amide protons to their H^{α} and H^{β}. Many of the H^{N}–H^{α} connections were established from the COSY spectrum shown in Figure 6. Because of overlap in the H^{α}, some of the H^{N} could not be unambiguously assigned. For several of these, TOCSY

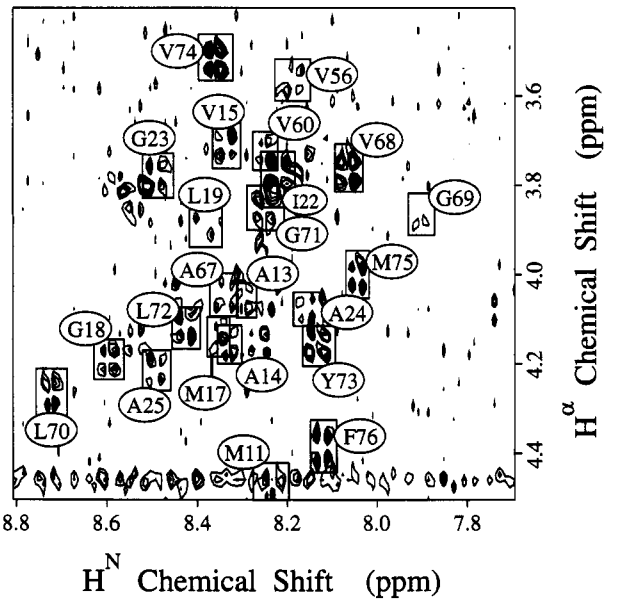

FIGURE 6: Fingerprint region of the DQF COSY spectrum of subunit *c*, showing the cross peaks between the H^{α} and the slowly exchanging H^{N} in ^2H solvent [2 mM in C^2HCl_3–$C^2H_3O^2H$–^2H_2O (4:4:1), 50 mM NaCl, pD 6.8].

and intraresidue NOE cross peaks between the H^{N} and H^{β} provided the H^{N} assignments.

Once the H^{N}–H^{α}–H^{β} sets had been established, we looked for the standard sequential NOESY connectivities: $d_{\alpha N}(i,i+1)$ for extended conformations, and $d_{NN}(i,i+1)$, $d_{\beta N}(i,i+1)$, $d_{\alpha N}(i,i+3)$, and $d_{\alpha\beta}(i,i+3)$ for α-helix, employing the usual notation (Wüthrich, 1986).[4] Figure 7 illustrates the H^{N}–H^{N} and H^{N}–H^{β} regions of the NOESY spectrum in ^2H solvent. The H^{N}–H^{N} and H^{N}–H^{α} regions are shown in Figure 8. Because of the broad line widths and the limited dispersion

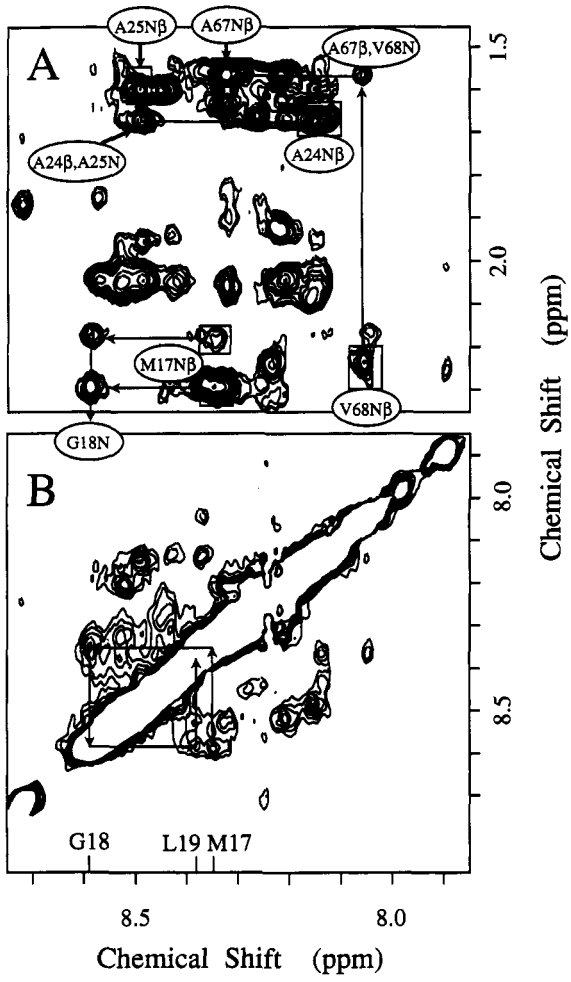

FIGURE 7: Expansions of the NOESY spectrum of subunit *c*, illustrating sequential connectivities between the slowly exchanging H^N and the H^N and H^β in ^2H solvent. (A) H^N–H^β region of the NOESY spectrum showing several example $d_{\beta N}$ connectivities in the N-terminal helix. Intraresidue cross peaks are enclosed in boxes with lines connecting them to the NOESY cross peak to the next residue. (B) H^N–H^N region showing the assignment spiral from d_{NN} connectivities for the Met17–Leu19 sequence. Conditions as in Figure 1, except that the NOESY pulse sequence with a 200-ms mixing time was used. The data were collected as 512 blocks of 128 transients.

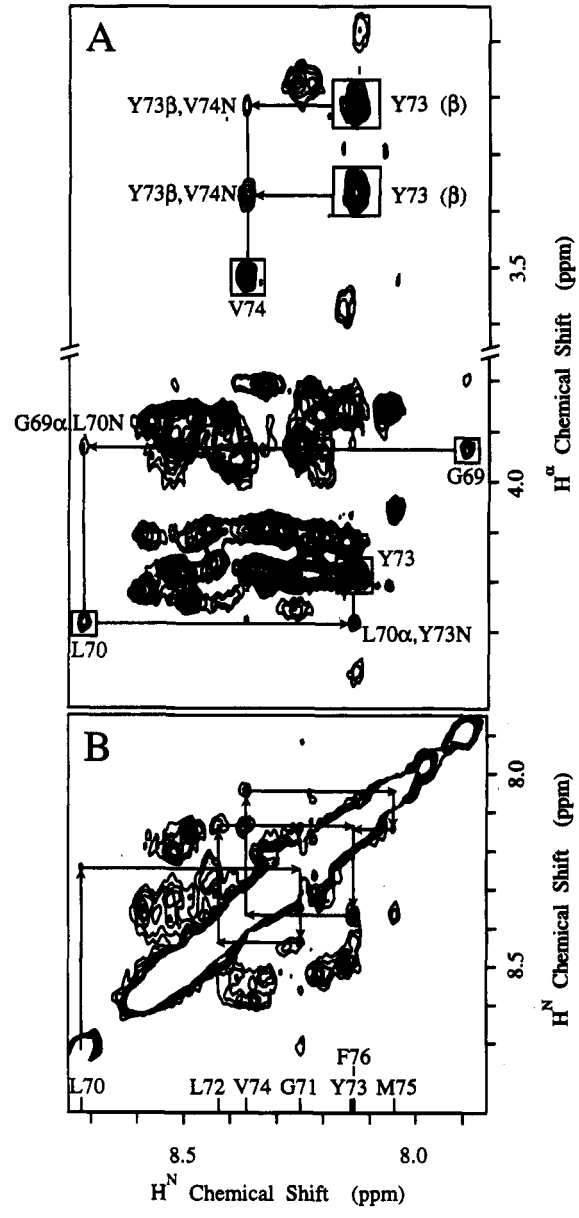

FIGURE 8: Expansions of the NOESY spectrum of subunit *c*, illustrating sequential connectivities between the slowly exchanging H^N and the H^N and H^α of the C-terminus of the protein in ^2H solvent. (A) H^N–H^α region of the spectrum illustrating an example $d_{\alpha N}(i,i+3)$ connectivity between Leu70 and Tyr73, a $d_{\alpha N}(i,i+1)$ connectivity between Gly69 and Leu70, and a $d_{\beta N}(i,i+1)$ between Tyr73 and Val74. Intraresidue cross peaks are enclosed in boxes with lines connecting them to the NOESY cross peak to the next residue. (B) H^N–H^N region showing the assignment spiral from d_{NN} connectivities for the Leu70–Phe76 sequence. Conditions as in Figure 7.

of the chemical shifts of the H^N resonances, the H^N–H^N cross peaks were relatively weak and often fell on or near the diagonal. For this reason, we often had to resort to $d_{\alpha N}(i,i+3)$, $d_{\beta N}(i,i+1)$, and $d_{\alpha\beta}(i,i+3)$ for the purpose of sequential assignment. The observed sequential NOESY connectivities are summarized in Figure 9.

(a) N-Terminal Helix. Several sequences of backbone NOE connectivities were observed for the region extending from Asp7 through Ala25 in the N-terminus of the protein (Figure 7). Two convenient starting points in this region were the unique Tyr10-Met11 pair linked via $d_{\beta N}$, and the Gly23-Ala24-Ala25 sequence linked via d_{NN} NOESY connectivities. From here, further connections were established, primarily involving short $i,i+3$ distances. Asp7 was assigned from the $d_{\alpha\beta}(i,i+3)$ cross peak to Tyr10. The $d_{\alpha\beta}(i,i+3)$ connection from Tyr10 to an Ala established the identity of Ala13. The Ala12-X-Ala14-Val15 sequence was established from the Ala12–Val15 $d_{\alpha\beta}(i,i+3)$ and the Ala14–Val15 $d_{\beta N}$. Met16 was assigned from the $d_{\alpha\beta}(i,i+3)$ between Ala13 and itself. Met17 and Gly18 exhibited both d_{NN} and $d_{\alpha N}$ connectivities. Leu19 was identified from the Gly18–Leu19 d_{NN} and a $d_{\alpha N}(i,i+4)$ from Val15. The H^β of Ile22 showed a $d_{\beta N}$ to Gly23. The Gly23 through Ala25 sequence exhibited strong d_{NN} and (except for Gly23) $d_{\beta N}$ connectivities. The Ala24 assignment was independently confirmed by analysis of an A24S mutant, where the H^α and H^β resonances were shifted to 4.64 and 3.82 ppm, respectively.

Two additional H^N–H^N connectivity sequences were observed which could not be rigorously assigned to an amino acid sequence. In the first, a sequence of four H^N–H^N connections beginning at an Ile and terminating at a Leu was present. This sequence probably corresponds to Ile28 through Leu31, but the side-chain types of the intervening two residues could not be defined due to degeneracy in the H^N chemical

[4] In this notation, *d* denotes a short distance giving rise to an NOE. N, α, and β give the location of the protons within the residue, and i, $i+1$, and $i+3$ are the relative sequential indices of the residues involved.

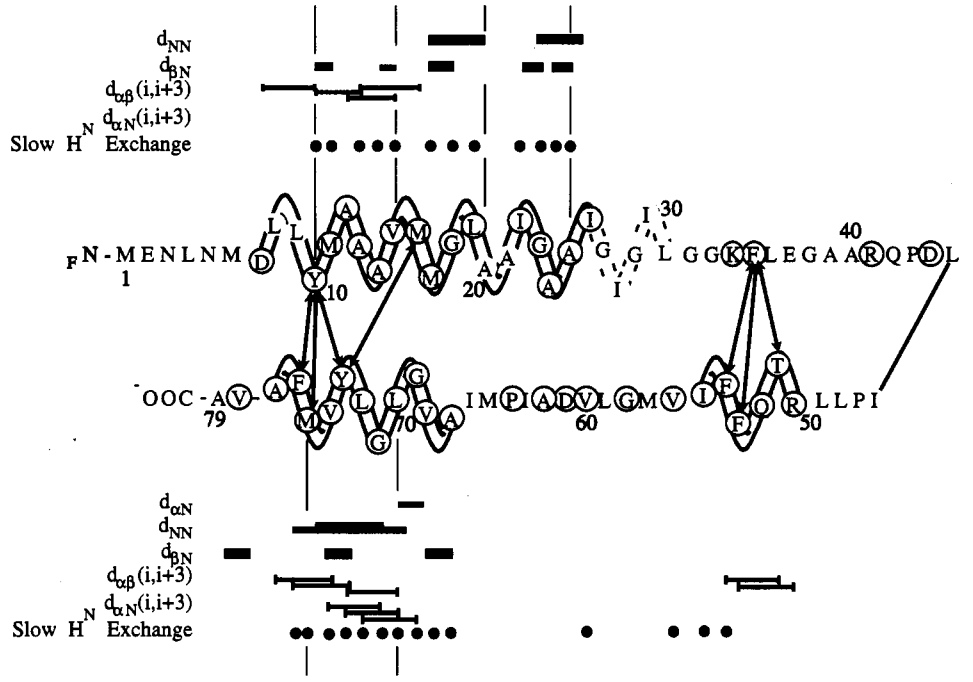

FIGURE 9: Summary of the observed sequential NOESY cross peaks seen in ^2H solvent. The thickness of the lines for $i,i+1$ connectivities is intended to approximate the intensity of the cross peak. NOESY cross peaks between helices are indicated by two-headed arrows connecting the residues involved. Also indicated are the H^N which exchanged slowly ($t_{1/2} > 1$ day), and the regions of α-helical secondary structure implied by the observed NOESY cross peaks. Sequential assignments are enclosed in circles. The helical segment drawn with dashed lines was tentatively assigned from an Ile-X-X-Leu d_{NN} series.

shifts. The H^N degeneracy persisted at pD 4.2. In the second, H^N–H^N and H^β–H^N NOEs occurred between two Ala. Presumably these are Ala20 and Ala21, since the H^N of other residues in this region exchange only slowly with ^2H solvent, but another pair of Ala occurs in the protein sequence at positions 39 and 40.

(b) C-Terminal Helix. A series of peptide backbone NOE connectivities was also observed in the C-terminal region of the protein as shown in Figures 8 and 9. An obvious starting point was the unique Tyr73-Val74 dipeptide, which exhibited strong d_{NN} and $d_{\beta N}$ cross peaks. The d_{NN} connectivities extended in the N-terminal direction through Leu72 and Gly71, to Leu70, and in the C-terminal direction through Met75 to Phe76. Ala77 was assigned via the $d_{\alpha\beta}(i,i+3)$ cross peak between Val74 and itself. At the other end of the sequence, Gly69 was identified from both its $d_{\alpha N}(i,i+1)$ cross peak to Leu70 and its $d_{\alpha N}(i,i+3)$ to Leu72. Ala67-Val68 were assigned from their sequential $d_{\beta N}$ connectivity.

Another stretch of helix occurs between residues 50 and 55, where the H^α of Arg50 and Thr51 were connected via $d_{\alpha\beta}(i,i+3)$ to the H^β of Phe53 and Phe54, respectively. The assignment of this last sequence also provided assignments for Arg41 and Phe35 by process of elimination, since these are the only remaining representatives of each of these residues. Val56 was identified by an NOE between the H^β of Phe54 and the Val H^N. Ile55 was assigned from an NOE between the Phe54 2,6 protons and the H^α of Ile55. It should be noted that the 2,6 ring protons of the three Phe and two Tyr residues in the assigned helical regions exhibited NOE cross peaks to both the H^α of residues $i+1$ and the H^α of residues $i-3$.

(c) Sequence Assignments around Asp61. The functionally crucial Asp61 was identified after modification with DCCD. Figure 4A shows the Asp $\alpha\beta$ proton regions of the COSY spectrum for unmodified subunit *c*, and Figure 4B shows the same region of the COSY spectrum for DCCD-modified subunit *c*. Several of the Asp and Asn cross peaks were altered somewhat in the DCCD-modified protein. The most striking effect is on the cross peak labeled as Asp61. This cross peak undergoes the largest changes in the chemical shifts for the α proton, and also a change in $^3J_{\alpha\beta}$ such that two H^α–H^β COSY cross peaks are observed, rather than just one.[5] Other effects of DCCD modification will be considered below.

Substitution of Glu for Asp at position 61 resulted in significant changes in the chemical shifts of a Val residue tentatively assigned as Val60. The H^β and H^γ resonances of the perturbed Val were shifted downfield by 0.05 and 0.03 ppm, while its H^α and the resonances for all other Val were unaffected (M. E. Girvin, F. Assadi, and R. H. Fillingame, unpublished data). Because of these changes, the residue was assigned as Val60, the residue adjacent to Asp61.[5] The only remaining Val was assigned as Val78.

NOEs between Helices in Purified Subunit c. The possible interactions between of the main sections of α-helix in the protein were of particular interest, because if found, such interactions could establish whether the purified protein was folded in a hairpin arrangement, as it does in the native F_o complex. Two factors prevented us from using NOEs between residues in helix-1 and helix-2 as a general method to determine 3D conformation: too many resonances were not yet sequentially assigned, and too many of the assigned protons resonated at frequencies too close to each other to be used without ambiguity. In spite of these limitations, several interhelical NOE connectivities were detected in the relatively uncrowded aromatic region of the NOESY spectrum (Figure 10). These include the following: five NOEs between the 2,6 ring protons of Phe35 and the H^α and H^γ of Thr51 (not shown), the H^β of Phe53, and the H^β and $H^{\beta'}$ of Phe54; five NOEs between the 2,6 ring protons of Tyr10 and the $H^{\beta'}$ of Tyr73, the H^α,

[5] In a complementary study (Girvin and Fillingame, in preparation), Asp61 has been specifically modified by a nitroxide analogue of DCCD, i.e., NCCD. Nitroxide-induced paramagnetic broadening resulted in the complete disappearance of resonances attributed here to Asp61, Val60, and Ala62, in support of the assignments given here.

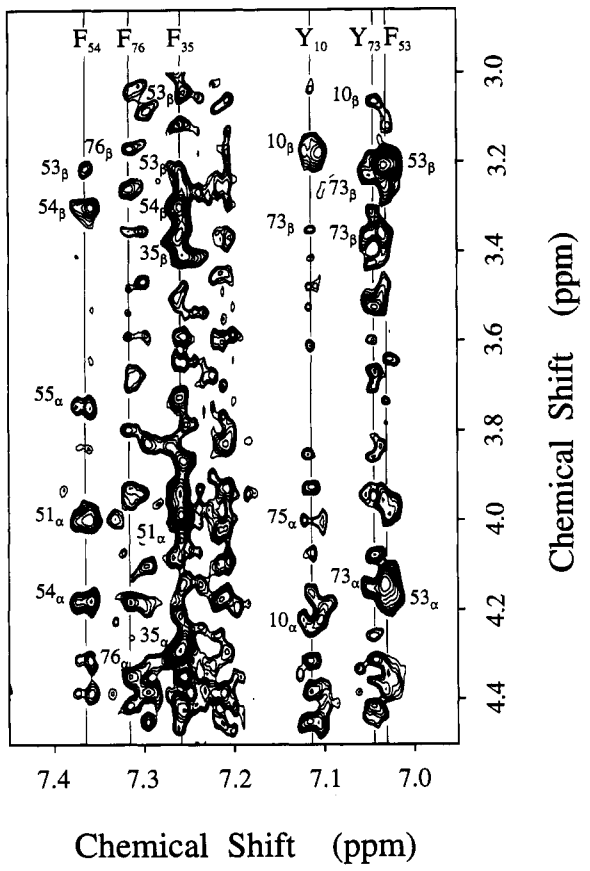

FIGURE 10: Region of the NOESY spectrum of subunit *c* showing cross peaks between aromatic ring protons and the H^{α} and aromatic H^{β} protons. Assigned NOEs are labeled to the left of the cross peak. Conditions are described in Figure 7.

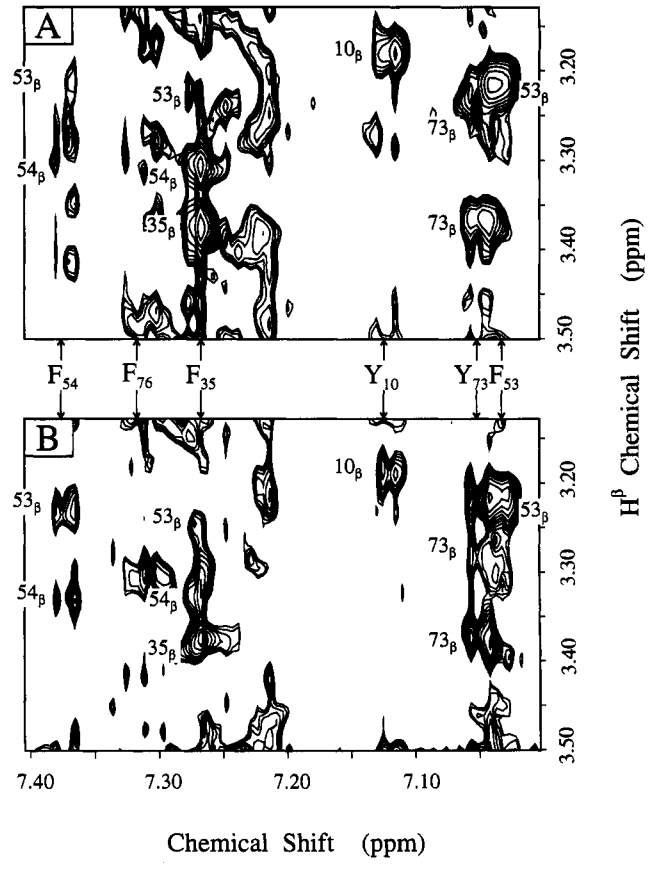

FIGURE 11: Comparison of aromatic NOE cross peaks in ^1H subunit *c* and a 1:1 mixture of ^1H subunit *c* with ^2H subunit *c*. Expansions of the aromatic ring proton to Phe and Tyr H^{β} regions of NOESY spectra for (A) ^1H subunit *c* and (B) 1:1 mixture of ^1H- and uniformly ^2H-labeled subunit *c*. Contour levels for (B) were plotted at twice the sensitivity of (A) to compensate for the reduced intensity from dilution with 50% ^2H. Aromatic proton chemical shifts are along the *x* axis. Cross peaks to H^{β} are labeled to their left (except for Phe53). In both spectra the total subunit *c* concentration was 2 mM. The mixing time used in the NOESY sequence was 150 ms, and 480 blocks of 64 transients were collected.

H^{γ}, and $H^{\gamma'}$ of Met75, and the H^{α} of Phe76; and two NOEs between the 2,6 protons of Tyr73, the H^{β} of Tyr10, and the H^{β} of Met16 (not shown).

Because of the oligomeric nature of subunit *c* in the F_o complex and its tendency to aggregate at higher concentrations in chloroform–methanol solvent lacking water, it was important to determine whether the observed NOEs arose from nearby side chains within a single subunit *c*, or between side chains on two associating subunits *c*. To distinguish between these two possibilities, the NOESY spectrum of a normal, ^1H preparation of subunit *c* was compared with that of a sample in which the ^1H protein had been mixed in a one-to-one ratio with uniformly deuterated subunit *c* (prepared from 99.8% ^2H growth medium). Any NOEs resulting from intermolecular interactions should be reduced by 50% in the ^2H dilution experiment. The regions of the NOESY spectra showing the NOEs between aromatic ring protons and the aromatic H^{β} are shown in Figure 11 for both samples. The signal-to-noise ratio of these two spectra is considerably lower than in the experiment shown in Figure 10 due to collection of fewer blocks (480 vs 512) of fewer transients (64 vs 128) because of limited spectrometer availability. All interhelical NOEs present in the ^1H control were also observed in the $^1H^2H$ spectrum, and no obvious diminutions of interhelical NOEs (e.g., Phe35 2,6H to Phe53 H^{β} and Phe54 H^{β}). This is most easily seen by comparing the intensity of interhelical NOEs to that of intrahelical NOEs (e.g., Phe54 2,6H to Phe53 H^{β}) or intraresidue NOEs (e.g., Phe54 2,6H to Phe54 H^{β}). The ratios of the volume integrals for several of the most easily measured NOE cross peaks are listed in Table II and, as stated above, were constant for both experiments.

Effects of DCCD Modification. Modification of Asp61 with DCCD does not appear to severely affect folding of the protein. The NOEs between the 2,6 protons of Phe35, and protons of Phe54 and Thr51 were still present in the DCCD-modified protein, so the protein must still fold as a hairpin. Many of the assigned cross peaks in the COSY spectrum were unaffected by DCCD modification; i.e., the observed changes in chemical shift were generally under 0.02 ppm (Figure 12A). It is of interest that the largest changes, secondary to those at Asp61 and Val60, occur at the N-terminus of helix-1 and at Asp44 in the polar loop.

The H^{α} and $(H^{\beta})_3$ of one Ala (AlaC) were shifted upfield by 0.14 and 0.05 ppm, respectively by DCCD modification. This Ala was first presumed to be Ala62, but COSY spectra of an A62S mutant (data not shown) clearly identify the resonances of Ala62 at 4.29, 1.58 ppm.[5] Since the AlaC resonances undergo the largest changes in chemical shift of any Ala on lowering the pH from 7 to 4.2, it may well be the C-terminal Ala79.

Helix–Helix Interactions in DCCD-Resistant Mutants of Subunit c. Two subunit *c* mutant proteins (Hoppe et al., 1980; Fillingame et al., 1991), in which substitutions in helix-1 reduce the rate of reaction of DCCD with Asp61 in helix-2 of native F_o, were studied. In the normally folded protein, where Asp61 is apparently positioned near residues 24 and 28, one might expect to see changes in the resonances of protons

Table II: Comparison of NOE Cross Peak Volumes in ^1H and Mixed $^1H^2H$ Samples

cross peak	NOE cross peak volume[a]		
	^1H sample	$^1H^2H$ sample	$^1H/^1H^2H$ ratio
	Intraresidue		
Y10 2,6H–Y10 H^α	1.036	0.429	2.41
Y10 2,6H–Y10 H^β	1.357	0.698	1.94
F35 2,6H–F35 H^α	2.000	0.996	2.01
F35 2,6H–F35 H^β	1.661	0.798	2.08
F54 2,6H–F54 H^α	1.344	0.624	2.15
F54 2,6H–F54 H^β	0.639	0.405	1.58
	intraresidue av:		2.03
	Intrahelical		
F54 2,6H–T51 H^α	0.707	0.490	1.44
F54 2,6H–F53 H^β	0.529	0.325	1.63
	intrahelical av:		1.53
	Interhelical		
Y10 2,6H–Y73 H^α	0.540	0.231	2.34
Y10 2,6H–Y73 H^β	0.185	0.122	1.52
Y10 2,6H–M75 H^α	0.392	0.203	1.93
Y10 2,6H–M75 H^γ	0.651	0.316	2.06
F35 2,6H–T51 H^α	1.174	0.564	2.08
F35 2,6H–F53 H^β	0.365	0.189	1.94
F35 2,6H–F54 H^β	1.088	0.530	2.05
	interhelical av:		1.99

[a] All cross peak volumes were normalized to a value of 2.0 for the F35 2,6H–F35 H^α cross peak.

near Asp61 on substitution at position 24 or 28. The differences in H^α and H^β chemical shifts between wild-type and the I28T and A24S mutants are shown in Figure 12B,C for the resonances which have been assigned. Substitution at either position 24 or 28 led to changes in chemical shift at the N-terminus of the protein (Asn3 through Val15), and in Asp44 in the polar loop. It is of interest that these effects mirror those caused by DCCD modification of Asp61 in the opposite helix. The I28T substitution caused significant changes in chemical shift for the protons of Asp61 and several of the neighboring residues in the DCCD binding region. The A24S substitution did not effect the resonances of Asp61, but did cause small changes in the proton resonances of neighboring residues.

DISCUSSION

Subunit *c* is thought to fold like a hairpin in the native F_o complex. The NMR experiments described in this paper show that purified subunit *c* also folds as a hairpin of two α-helices in chloroform–methanol–water solution. Interhelix NOEs were observed at both ends of the two helices, and these interactions were shown to occur between residues within a single subunit *c*. It would appear that the helices lie in parallel for most of their length. Such a model differs from the wedge-like structure proposed by Fimmel et al. (1983), where a bend in helix-2 was proposed at Pro64, a residue thought to be essential to the function of the protein. Our own model building suggests that the two helices are gently twisted around one another, with the C-terminal helix being more curved than the N-terminal helix (Girvin and Fillingame, in preparation). The Pro at position 64 contributes to the greater curvature of the C-terminal helix.

The effect of the I28T substitution on the chemical shifts of Val60 and Asp61 supports the conclusion that the purified protein folds with a native-like structure. In the native F_o complex, this substitution greatly reduces the DCCD reactivity of Asp61 (Hoppe et al., 1980; Fillingame et al., 1991). In experiments to be described elsewhere we have shown that

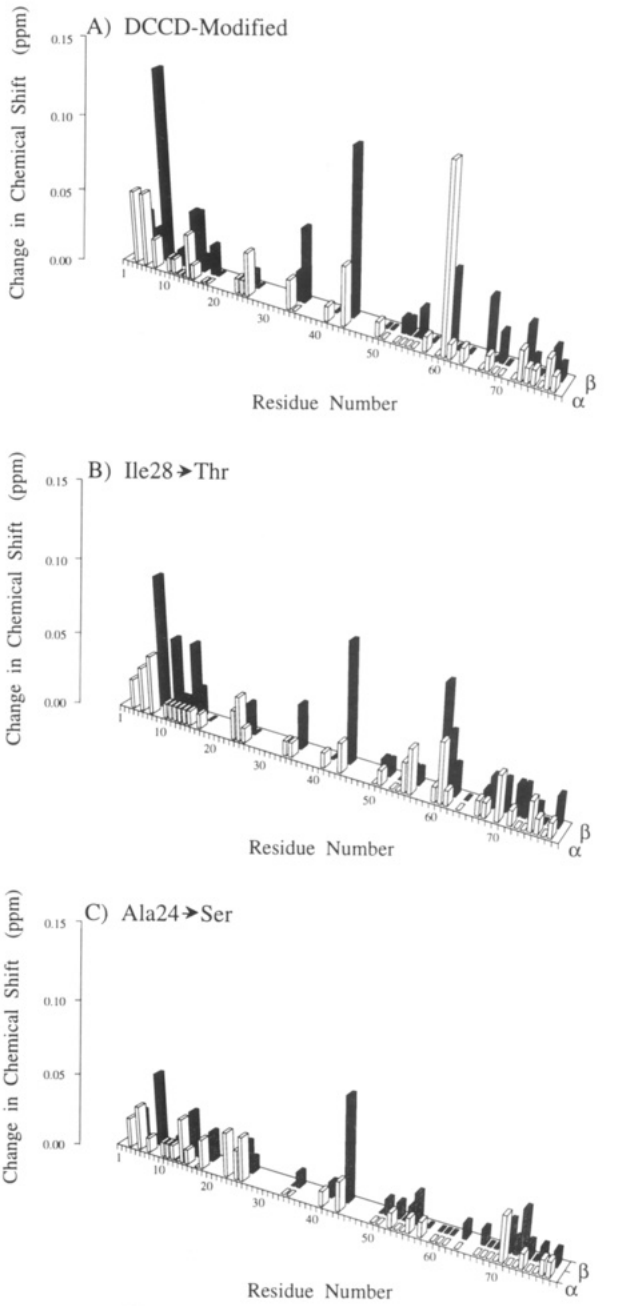

FIGURE 12: Differences in chemical shifts for DCCD-modified and mutant subunit *c* relative to the wild-type protein. (A) DCCD-modified subunit *c*, (B) I28T subunit *c* mutant, and (C) A24S subunit *c* mutant. Plotted are the absolute values of the differences in chemical shift between the wild-type and the altered protein for both the H^α (open bars) and H^β (hatched bars).

the unique chemical reactivity of Asp61 with DCCD is preserved in the purified protein and that Asp61 of the I28T protein is less reactive to DCCD than Asp61 of the wild-type protein. Further support for the hairpin folding model is provided by experiments in which Asp61 is modified with a paramagnetic nitroxide analog of DCCD (NCCD). The piperidyl (nitroxide) ring of NCCD is shown to lie between the Asp61 region of helix-2 and Ala24 and Ile28 of helix-1 (Girvin and Fillingame, in preparation).

This study demonstrates an α-helical conformation for the Asp7–Ala25, Arg50–Ile55, and Ala67–Ala77 sequences of the protein in [^2H]chloroform–methanol–water solvent. The H^N in these regions exchange very slowly with D_2O. Our preliminary experiments in protic solvent indicate that another 20 residues may be in an α-helical conformation. These results

confirm previous predictions of a largely α-helical conformation (65–80%) for subunit *c*, based upon circular dichroism measurements on the protein in trifluoroethanol, detergent micelles, and liposomes (Hoppe & Sebald, 1982; Mao et al., 1982). It is of interest that the locations of the helical segments provided by the ^{1}H NMR measurements correspond to regions that were proposed to be helical in the membrane according to labeling with 3-(trifluoromethyl)(3-*m*-iodophenyl)diazirine. This hydrophobic, light-activated carbene gave a roughly *i*,*i*+3 modification pattern for Leu8 through Leu19, Phe53 and Met57, and Tyr73 and Phe76. Such a labeling pattern might be expected for helical segments in which only one face is exposed to the hydrophobic phase of the lipid bilayer (Hoppe et al., 1984).

The striking similarities between purified subunit *c* and the protein in the native F_o complex may seem somewhat surprising. The driving force to fold as a helical hairpin might be expected to differ for a protein in chloroform–methanol–water versus a protein in a lipid bilayer separating two aqueous compartments. The solvent mixture may be crucial to the folding since the distribution of water around hydrophobic versus polar surfaces of the protein may vary. The properties of the protein in chloroform–methanol solution lacking water do differ significantly as discussed below.

In an earlier NMR study of subunit *c*, Moody et al. (1987) provided preliminary evidence that the isolated protein might be largely α-helical and that it might fold in a hairpin arrangement. The conclusion that the protein adopted a largely α-helical structure was based on the observation of H^N–H^N NOESY connectivities, and on the inability to measure any of the $^3J_{HN} \approx 9$ Hz coupling constants expected for extended structures. Hairpin folding was inferred from the effects of paramagnetic shift reagents (lanthanides), which were postulated to bind exclusively at the C-terminus of the protein. The binding of the lanthanides affected the chemical shifts of both Tyr73 in the C-terminus and Tyr10 in the N-terminus, but not residues in the polar loop (e.g., Thr51). Because of the relative broadness and overlap of the resonances, only a few sequence-specific assignments were made (Thr51, and tentative assignments for Tyr10, Tyr73, Ala77, Val78, and Ala79).

One concern raised in the study of Moody et al. (1987) was the possibility of protein aggregation. Also, only one group, the carboxyl of the tentatively assigned C-terminal Ala79, was found to ionize over a pH range of 2–9, despite the presence of 3 Asp, 2 Glu, 2 Arg, and 1 Lys residues in the protein. The solvent system used by Moody et al. was composed of only chloroform and methanol, usually 2:1 or 1:1. We chose not to use this solvent system because of protein concentration-dependent line broadening that we attribute to subunit–subunit association. In the present study the solvent consisted of chloroform–methanol–water (4:4:1) made 50 mM in NaCl. Sharp resonances that were not subject to concentration-dependent broadening were observed. A second difference in properties of the protein in this solvent mixture is that we have observed pH-dependent changes in chemical shift for all Asp groups, between pH 4 and 8.5 (F. Assadi, M. Girvin, and R. Fillingame, unpublished data). That the addition of water and salt to the solvent should affect aggregation, conformation, or ionization is not surprising. In one of the purification steps, the protein is bound to CM-cellulose in chloroform–methanol (2:1), despite an expected net negative charge if all carboxyl groups were ionized. The protein can then be washed from this matrix with chloroform–methanol–water (4:4:1). A change in conformation of subunit *c*, on adding water to the protein dissolved in organic solvents, was also observed in the circular dichroism measurements of Hoppe and Sebald (1982).

Subsequently, Norwood et al. (1992) published a $^1H^{15}N$ NMR analysis of protein backbone assignments and secondary structure of subunit *c* dissolved in trifluoroethanol. The NMR evidence suggested long α-helical segments between residues 10–40 and residues 48–76. Because of the differences in experimental conditions, it is difficult to compare their assignments and secondary structure directly to our own. Their experiments were carried out at 47 °C at pH 4.8 in trifluoroethanol (presumably without any salts), and the reference compound for chemical shifts was not given. The ^{1}H chemical shifts do differ from our own by up to 0.5 ppm. In contrast to the observations of Moody et al. (1987), made with protein in chloroform–methanol solvent, Norwood et al. reported that the 3 Asp and 2 Glu titrated with pK_a's ≤5.5 in trifluoroethanol. No evidence of long-range interactions between helical segments was reported due to problems with spectral overlap. It thus remains unclear whether subunit *c* folds in a hairpin-like structure in trifluoroethanol as it does in the chloroform–methanol–H_2O solvent used here.

Major changes in the polar loop region of the protein were observed after DCCD modification of Asp61. The loop is thought to function in the coupling of proton translocation through F_o to ATP synthesis/hydrolysis in F_1. The changes observed may relate to the inhibition of coupled ATPase activity brought about by the DCCD modification. It is of interest that the A24S and I28T forms of the protein also exhibited changes in the loop region, in that these substitutions enhance coupled ATPase activity (Fillingame et al., 1991). Changes in the chemical shift of polar loop residue ^{1}H's are also observed on substitution of Glu for Asp61, and during the titration of Asp61 with H^+ (F. Assadi, M. E. Girvin, and R. H. Fillingame, unpublished results). In summary, a variety of minor structural changes at or around Asp61 result in global changes in subunit *c* structure. Such properties might be expected of a protein involved in conformational coupling.

Future work will be directed at providing more detailed information about the conformation of the remainder of the protein. Preliminary NOESY spectra in ^{1}H solvent do indicate that 10–20 more residues are part of α-helices, on the basis of the observed d_{NN} connectivities, and at least 10 residues show the strong $H^\alpha(i)$–$H^N(i+1)$ connectivities indicative of extended conformations. We have observed two $H^\alpha(i)$–$H^\beta(i+3)$ NOESY cross peaks which were consistent with the sequence from Gly32 through Ala40 being α-helical, but the assignments of these four residues have not been independently confirmed by sequential H^N NOE connectivities. Because of the extensive crowding in H^N chemical shifts, we feel we have gone as far as possible with 2D NMR techniques. Further progress will require the use of 3D and 4D NMR techniques to complete the sequential assignments and assign the interresidue NOEs necessary for defining the structure of the protein.

ACKNOWLEDGMENT

The NMR experiments were carried out at the National Magnetic Resonance Facility at Madison. We thank its director, Professor John Markley, and Drs. Ed Mooberry, Eldon Ulrich, and Milo Westler for their interest and essential advice on spectroscopy. We thank Fariba Assadi and Joseph Hermolin for preparation of DCCD-labeled subunit *c* and Mary Gillis for excellent general assistance and help in growth and purification of ^{2}H-subunit *c*.

REFERENCES

Bax, A., & Davis, D. G. (1985) *J. Magn. Reson. 65*, 355–360.
Beechey, R. B., Linnett, P. E., & Fillingame, R. H. (1979) *Methods Enzymol. 55*, 426–434.
Bodenhausen, G., Kogler, H., & Ernst, R. R. (1984) *J. Magn. Reson. 58*, 370–388.
Felton, J., Michaelis, S., & Wright, A. (1980) *J. Bacteriol. 142*, 221–228.
Fillingame, R. H. (1975) *J. Bacteriol. 124*, 870–883.
Fillingame, R. H. (1976) *J. Biol. Chem. 251*, 6630–6637.
Fillingame, R. H. (1990) in *The Bacteria* (Krulwich, T. A., Ed.) Vol. XII, pp 345–391, Academic Press, New York.
Fillingame, R. H., Peters, L. K., White, L. K., Mosher, M. E., & Paule, C. R. (1984) *J. Bacteriol. 158*, 1078–1083.
Fillingame, R. H., Oldenburg, M., & Fraga, D. (1991) *J. Biol. Chem. 266*, 20934–20939.
Fimmel, A. L., Jans, D. A., Langman, L., James, L. B., Ash, G. R., Downie, J. A., Senior, A. E., Gibson, F., & Cox, G. B. (1983) *Biochem. J. 213*, 451–458.
Foster, D. L., & Fillingame, R. H. (1982) *J. Biol. Chem. 257*, 2009–2015.
Fraga, D., & Fillingame, R. H. (1989) *J. Biol. Chem. 264*, 6797–6803.
Girvin, M. E., Hermolin, J., Pottorf, R., & Fillingame, R. H. (1989) *Biochemistry 28*, 4340–4343.
Graf, T., & Sebald, W. (1978) *FEBS Lett. 94*, 218–222.
Hensel, M., Deckers-Hebestreit, G., Schmid, R., & Altendorf, K. (1990) *Biochim. Biophys. Acta 1016*, 63–70.
Hermolin, J., & Fillingame, R. H. (1989) *J. Biol. Chem. 264*, 3896–3903.
Hermolin, J., Gallant, J., & Fillingame, R. H. (1983) *J. Biol. Chem. 258*, 14550–14555.
Hoppe, J., & Sebald, W. (1982) in *Chemistry of Peptides and Proteins*, (Voelter, W., Wünsch, E., Ovchinnikov, J., & Ivanov, V., Eds.) Vol 1, pp 489–498, Walter de Gruyter & Co., Berlin.
Hoppe, J., & Sebald, W. (1984) *Biochim. Biophys. Acta* 768, 1–27.
Hoppe, J., Schairer, H. U., & Sebald, W. (1980) *Eur. J. Biochem. 112*, 17–24.
Hoppe, J., Schairer, H. U., Friedl, P., & Sebald, W. (1982) *FEBS Lett. 145*, 21–24.
Hoppe, J., Brunner, J., & Jørgensen, B. B. (1984) *Biochemistry 23*, 5610–5616.
Klionsky, D. J., Brusilow, W. S. A., & Simoni, R. D. (1983) *J. Biol. Chem. 258*, 10136–10143.
Kumar, A., Ernst, R. R., & Wüthrich, K. (1980) *Biochem. Biophys. Res. Commun. 95*, 1–6.
Macura, S., Wüthrich, K., & Ernst, R. R. (1982) *J. Magn. Reson. 46*, 269–282.
Mao, D., Wachter, E., & Wallace, B. A. (1982) *Biochemistry 21*, 4960–4968.
Messing, J., & Vieira, J. (1982) *Gene 19*, 269–276.
Miller, M. J., Fraga, D., Paule, C. R., & Fillingame, R. H. (1989) *J. Biol. Chem. 264*, 305–311.
Miller, M. J., Oldenburg, M., & Fillingame, R. H. (1990) *Proc. Natl. Acad. Sci. U.S.A. 87*, 4900–4904.
Moody, M. F., Jones, P. T., Carver, J. A., Boyd, J., & Campbell, I. D. (1987) *J. Mol. Biol. 193*, 759–774.
Mosher, M. E., White, L. K., Hermolin, J., & Fillingame, R. H. (1985) *J. Biol. Chem. 260*, 4807–4814.
Norwood, T. J., Crawford, D. A., Steventon, M. E., Driscoll, P. C., & Campbell, I. D. (1992) *Biochemistry 31*, 6285–6290.
Porter, A. C. G., Brusilow, W. S. A., & Simoni, R. D. (1983) *J. Bacteriol. 155*, 1271–1278.
Rance, M., Sørensen, O. W., Bodenhausen, G., Wagner, G., Ernst, R. R., & Wüthrich, K. (1983) *Biochem. Biophys. Res. Commun. 117*, 479–485.
Schneider, E., & Altendorf, K. (1985) *EMBO J. 4*, 515–518.
Sebald, W., & Hoppe, J. (1981) *Curr. Top. Bioenerg. 12*, 1–64.
Sebald, W., Machleidt, W., & Wachter, E. (1980) *Proc. Natl. Acad. Sci. U.S.A. 77*, 785–789.
Senior, A. E. (1988) *Physiol. Rev. 68*, 177–231.
Wüthrich, K. (1986) *NMR of Proteins and Nucleic Acids*, Wiley, New York.